

Article

# Investigation of Heat Transfer Properties of Plasma-Treated and Silicone-Elastomer Coated Basalt Fabric

Meiling Zhang <sup>1,2</sup>, Ron Denning <sup>3</sup> , Zhili Zhong <sup>1</sup>, Xungai Wang <sup>2</sup>, Yiwen Shen <sup>1</sup> and Maryam Naebe <sup>2,\*</sup> 

<sup>1</sup> School of Textile Science and Engineering, Tianjin Polytechnic University, Tianjing 300387, China; zhangmeiling@tjpu.edu.cn (M.Z.); zhongzhili@tjpu.edu.cn (Z.Z.); sevenyiwen@163.com (Y.S.)

<sup>2</sup> Institute for Frontier Materials, Deakin University, Geelong, Victoria 3216, Australia; xungai.wang@deakin.edu.au

<sup>3</sup> CSIRO Manufacturing, Geelong Victoria 3216, Australia; Ron.Denning@csiro.au

\* Correspondence: maryam.naebe@deakin.edu.au; Tel.: +61-3-5227-2783

Received: 29 March 2019; Accepted: 25 April 2019; Published: 28 April 2019



**Abstract:** In this study, the effect of pre-plasma treatment on the adsorption of silicone to enhance the heat transfer resistance of basalt fabric for protective clothing was investigated. Fabrics were treated with plasma prior to surface coating. Changes to the un-sized basalt fibre surface were characterized by using scanning electron microscopy (SEM), scanning probe microscopy (SPM), X-ray photoelectron spectroscopy (XPS), and contact angle measurement. Furthermore, heat transfer and scanning electron microscopy (SEM) of basalt fabric coated with silicone were assessed. The results show that the different percentage add-ons of silicone had a significant effect on the heat transfer rate of the un-sized basalt fabric. Plasma treatment changed the fibres physically and enhanced the uniformity of the silicone coating. A combination of the plasma treatment and silicone coating revealed a significant difference in the heat transfer rate compared to the silicone-only coated basalt fabric. This finding can potentially be used to both engineer and tune the performance of protective clothing.

**Keywords:** basalt; plasma; heat transfer; coating; silicone; protective clothing

## 1. Introduction

Basalt fibres are environmentally friendly, non-hazardous materials containing 45%–52% SiO<sub>2</sub>. Fibres are continuously extruded from a high-temperature melt of basalt stone. The resulting basalt fibres have excellent properties such as high-modulus, high-heat and sound insulation, and high-heat resistance and thermal stability. Basalt fibres are also less prone to damage from alkali, acid solution, and water [1–3]. These excellent properties facilitate many potential applications including infrastructure [4], the automotive industry, and consumer products for basalt fibres and fabrics.

For many of these applications, researchers have used basalt fibre as a reinforcing material. Mechanical characterization of basalt fibre-reinforced plastic has shown that the fibres can be used in fields where glass composites are largely applied [5]. Meng et al. reported an experimental and numerical study of a basalt fibre cloth-strengthened, structural insulated panel, under the impact of windborne debris. The results indicate that basalt fibre cloth enhanced the impact resistance of the oriented strand board (OSB) structural insulated panel (SIP) [6]. Carmisciano et al. performed a comparative study of basalt and E-glass woven fabric-reinforced composites. The results showed that basalt fibres are promising as reinforcement in polymer matrix composites in comparison to E-glass composites [1].

The flexural behaviour of engineered cementitious composites and concrete beams reinforced with basalt fibre-reinforced polymer bars were numerically investigated. According to the simulation results, the basalt fibre-reinforced, polymer-reinforced engineered cementitious composite (ECC) beams show much better flexural properties in terms of load-carrying capacity, deformability, and crack controlling ability compared to the basalt fibre-reinforced polymer-reinforced concrete beams [7].

Different amounts of chopped basalt fibres were added to recycled concrete aggregate. Increasing the content of chopped basalt fibre significantly improved both the splitting tensile strength and the flexural strength of concrete [8]. The immobilization on the cylindrical surface of basalt fibres using two-dimensional graphene oxide flakes was described. The results showed that immobilization of graphene oxide flakes on the cylindrical surface of basalt fibres was feasible by using an electrostatic technique [9]. The low-velocity impact response of homogenous basalt fibre-reinforced polymer composites was studied, and the impact of key parameters were compared to carbon fibre-reinforced polymer homogenous composites. Better low-velocity impact performance was observed for basalt fibre-reinforced polymer compared to that of carbon fibre-reinforced polymer [10].

There is growing interest in using basalt fibre for high-temperature applications. Basalt fibre's operating temperature limit is 650 °C with a softening temperature of 1050 °C. Therefore, basalt fibre is being considered for use in high-temperature applications, such as in hot gas filtration systems [11] and fire-resistant electrical cable systems [12].

The effect of high temperatures on the bonding performance of fibre-reinforced polymer bars in concrete was studied [13]. The bond strength gradually declined with the increasing temperature. However, the effect of temperature on the bond strength of the glass fibre-reinforced polymer bar was greater than that of the basalt fibre-reinforced polymer bar. The mechanical properties of basalt fibre-roving and pultruded basalt fibre-reinforced polymer plates were studied at elevated temperatures. The results showed that the basalt fibre-roving and basalt fibre-reinforced polymer plates had much better tensile properties and temperature resistance compared to the glass fibre [14]. Bhat et al. investigated the fire resistance of a basalt fibre-reinforced polymer composite. When exposed to the same radiant heat flux, the basalt fibre composite heated up more rapidly and reached higher temperatures than the glass fibre laminate due to its higher thermal emissivity [2].

Modification of the surface of basalt fibres by acid treatment has been reported [15]. However, using these chemicals is not environmentally friendly. Therefore, a more ecologically desirable method is required to be adopted to reduce the use of toxic chemicals. Plasma technology is a dry and environmental friendly method that can alter up to 4–10 nm depth of the surface of a material, but does not modify the bulk properties [16,17]. Different functional groups can be introduced on the fibre surface using a range of conditions and monomers. The hydrophilicity and roughness of a surface can be changed. Kurniawan et al. treated basalt fibre and polylactic acid composites with plasma and analysed the mechanical properties [18]. Kim et al. studied the effect of plasma treatment on the tribological behaviour of basalt and epoxy woven composites. Oxygen plasma treatment of basalt fibres improved the interfacial adhesion between the fibre and resin [19], and argon/propane-butane low-temperature plasma treatment increased the maximum breaking load of basalt fibres compared to untreated fibres [20]. The basalt fibre and polylactic acid composite's strength and modulus were higher compared to those of the untreated control after the application of atmospheric-pressure glow discharge plasma [18]. The adhesive force between fibre and resin was improved by low-temperature atmospheric oxygen plasma treatment, and this increased the interlaminar fracture toughness of basalt and epoxy woven composites [21,22].

There are very few studies in the development of personal protective clothing [23], including wildland firefighting gear, which use basalt fibres or fabrics. Firefighter protective clothing is not intended to provide protection during fire entrapment, according to the standard ISO 15384:2003 [24], MOD, but is designed to be used for extended periods during wildland fire-fighting and associated activities. Wildland fire-fighting involves working primarily in summer temperatures for many hours, which results in the generation of high-levels of metabolic heat and the firefighter may develop heat

stress. Consequently, the protective clothing should be light, flexible, and commensurate with the risks to which the firefighter may be exposed in order to be effective without introducing heat stress to the wearer. This international standard does not cover clothing for use in high-risk situations where clothing complying with ISO 11613 [25] or ISO 15538 [26] is more suitable. This international standard also does not cover clothing to protect against chemical, biological, electrical, or radiation hazards.

While the mechanical requirements of protective clothing can be easily satisfied due to the high-modulus of basalt fibre, heat transfer (radiation), and water vapour resistance, the two other main indexes essential for protective clothing are required to be improved. Basalt fabric has a tendency to be itchy due to the brittleness of the fibres, which is not suitable for clothing in contact with the skin.

Coating the surface of the fabric with silicone may reduce this problem while possibly also improving the radiant heat transfer of the basalt fabric. However, there is a gap in knowledge for understanding the chemical and physical changes plasma treatment produces at the surface of basalt fibre and how these changes promote adhesion between basalt and silicone. In addition, there is very little, if any literature on the application of silicone to plasma treated basalt to enhance the heat transfer resistance of basalt fabric. Therefore, this study aims to investigate if the application of silicone can satisfy the minimum heat transfer requirements for firefighters' protective clothing. The effect of pre-plasma treatment on the coating of silicone on basalt fabric is also investigated.

## 2. Materials and Methods

A commercial, plain-weave pure basalt fabric made of 116 tex basalt untwist roving, with a weight of 204 g/m<sup>2</sup> (made by Sichuan Aerospace Tuoxin Basalt Industrial Co., Ltd., Chengdu, China) was used. The fibre diameter was 9 µm. Untreated fabric samples were soaked in ethanol in a sealed vessel for 48 h, dried in a fume hood for 2 h, and then the un-sized fabrics were conditioned for 24 h under standard conditions (20 ± 2 °C, 65% ± 2% RH) prior to the plasma treatment and X-ray photoelectron spectroscopy analysis.

### 2.1. Plasma Treatment

A vacuum plasma was used to treat 200 mm × 200 mm fabric samples. The chamber was evacuated (Granville-Phillips 307 Vacuum Gauge Controller, MKS Instruments, Inc., Andover, MA, USA), then operated with 1 min of argon and 5 min of oxygen as the plasma gas. The pressure was between 0.05 and 0.08 mbar with the base pressure of 0.05 mbar. The operating pressure of argon was 0.063 mbar and for oxygen it was 0.066 mbar. Fabrics were treated using a 200-watt radio frequency power generator (Model Cesar, Advanced Energy, Fort Collins, CO, USA).

### 2.2. Silicone-Elastomer Coating

Silicone, Bluesil RTV 3428 A and B (Elkem, Bluestar Company, Lyon, France), a two-component silicone-elastomer that cures at room temperature by a polyaddition reaction with a pot-life of 60 min, was applied to fabric samples using an Ernst Benz (Germany) model GST-500 hand laboratory coater () fitted with a shoe blade in blade-over-roll configuration and a blade angle of 90°. The coating add-on per unit area was controlled by adjusting the height of the blade between 0.5 and 0.7 mm. Un-sized and plasma-treated fabric samples were coated with the mixture of Bluesil RTV 3428 A and B (Elkem) (in a weight ratio of 10:1). Silicone coating of the plasma-treated fabrics was carried out within 5 h of plasma treatment. The samples were then cured at ambient conditions for 24 h and then conditioned for 24 h prior to characterisation and testing.

The aim of the coating was to control the add-on of polymer rather than the thickness of the coated sample. The silicone coating add-on (CR (%)) was calculated using a fabric size of 200 × 200 mm<sup>2</sup> and the following equation:

$$\text{CR (\%)} = 100 \times (W_C - W_{UC})/W_{UC} \quad (1)$$

where  $W_C$  was the fabric's mass per unit area after coating with silicone ( $\text{g/m}^2$ ), and  $W_{UC}$  was the fabric's mass per unit area with no silicone ( $\text{g/m}^2$ ).

### 2.3. Thickness Measurements

Fabric thickness after the silicone coating was measured using a Mercer Model 110 thickness gauge (New York, NY, USA) with a 9.436 g dead load and 10 mm diameter foot. Fabric thickness was measured at a minimum of 5 random locations on the fabric.

### 2.4. Radiant Heat Transfer Evaluation

Heat transfer was evaluated using Method B of ISO 6942:2002 [27]. The test specimen was fastened to one side plate of the specimen holder and held in contact with the face of the calorimeter, applying a force of 2 N. The calorimeter was fixed in position behind the shutter of the vertical test frame. The radiation source was positioned at a distance such that the required incident heat-flux density of  $40 \text{ kW/m}^2$  irradiated the sample. The temperature monitor was switched on and the shutter between the source and the sample was opened. The shutter was closed after the calorimeter temperature had increased by more than  $24 \text{ }^\circ\text{C}$ . The sample size needed for the radiant heat test is ideally  $200 \text{ mm} \times 90 \text{ mm}$ .

A fabric or assembly is considered to pass the heat transfer test if the following results are achieved:

$$t_{24} \geq 11 \text{ s}, T_F \leq 70\%, \text{ and } t_{24} - t_{12} \geq 4 \text{ s} \quad (2)$$

where  $T_F$  is the heat transmission factor,  $t_{12}$  is the time for a temperature rise of  $12 \pm 0.1 \text{ }^\circ\text{C}$ , and  $t_{24}$  is the required time for a temperature rise of  $24 \pm 0.2 \text{ }^\circ\text{C}$  on the calorimeter face. The greater the differences between  $t_{24}$  and  $t_{12}$ , the better the insulation.  $T_F(Q_0)$  is given by the equation,  $T_F(Q_0) = \frac{Q_C}{Q_0}$ , where  $Q_0$  is the incident heat-flux density.  $Q_C$  is the transmitted heat-flux density in  $\text{kW/m}^2$ .

### 2.5. Scanning Electron Microscopy (SEM)

Surface morphology of the basalt fabric samples was studied using a thermal field emission scanning electron microscope (ZEISS Gemini SEM 500, Jena, Germany). The images were taken at a working distance of 10.8 mm, an accelerating voltage of 10.0 kV, and 5000 times magnification. Basalt fabric samples were gold-coated before imaging, using a coating unit (Hitachi High-Tech Science Systems Corporation, E-1045, Tokyo, Japan).

Some coated fabrics were sectioned using single-use, Diplomat brand, PTFE-coated, stainless-steel injector blades (ProSciTech, Kirwan QLD, Australia). The sections were then mounted on aluminium sample holders using double-sided adhesive carbon tape (ProSciTech, Kirwan, QLD, Australia). The samples were then coated with 3 nm of a Pt/Pd alloy using a Cressington 208 HRD magnetron coater (Cressington Scientific Instruments, Watford, UK). Imaging (secondary electron) of these samples was carried out using a Hitachi S4300 SE/N Field Emission Scanning Electron Microscope (Hitachi, Tokyo, Japan) with an incident beam-energy of 2 kV, a nominal working distance of 10 mm, a condenser lens setting of 12 and a  $20 \text{ }\mu\text{m}$  objective aperture in high-vacuum mode.

### 2.6. Scanning Probe Microscopy (SPM)

Fibres were withdrawn from un-sized and plasma-treated fabric, where the selection was from both warp and weft areas, and fibres were mounted on a microscope slide using double-sided adhesive tape. A CSPM 5500 scanning probe microscope (Benyuan Nanometer Instrument Co., Ltd., Beijing, China) was used to scan and analyse the three-dimensional surface of basalt fibres before and after plasma treatment. Tapping mode was selected to scan the samples, using a resolution of 512, 1 HZ frequency, and a 2000 nm scanning range.

### 2.7. X-ray Photoelectron Spectroscopy (XPS)

Basalt samples were analysed using an axis ultra-photoelectron spectroscopy (PHI 5000 VersaProbe Scanning ESCA Microprobe, Makasaki, Japan) equipped with a monochromatic X-ray source (Al K $\alpha$ ,  $h\nu = 1486.6$  eV), operating at 44.9 W. The analysis depth was 2–10 nm. Survey spectra were acquired for binding energies of 0 to 1400 eV, using a pass energy of 187.85 eV. High-resolution spectra were acquired using a pass energy of 46.95 eV. Spectra were charge-corrected with reference to the C 1s signal (284.8 eV). The estimated errors were  $\pm 10\%$ .

### 2.8. Assessment of Wettability

The hydrophobic and the hydrophilic properties of the basalt fabric were assessed using water contact angle and water absorption times, which were tested using a KSV CAM 200 contact angle instrument (KSV Instruments Ltd., Helsinki, Finland). Liquid drops with a volume of 3.65  $\mu\text{L}$  were placed on each sample with a pipette, and the image of each drop was captured as quickly as possible after the drops were deposited. The average of 3 measurements are reported for each sample [28]. Work of adhesion ( $W$ ) between water and the fibre surface was estimated using the Young-Dupré equation:

$$W = \gamma (1 + \cos \theta) \quad (3)$$

where  $\gamma$  is the surface tension of water at 20 °C and  $\theta$  is the contact angle in degrees.

## 3. Results and Discussion

### 3.1. Fabric Heat Transfer Assessment

Table 1 shows the mass per unit area of fabric samples before and after coating with silicone and their calculated silicone content (CR (%)). Fabric thickness after silicone coating is also shown in Table 1 for selected sample pairs with matched silicone add-ons of nominally 175% and 260%. Silicone add-ons range between 100% and 290%. Increasing the blade height had little effect on the final fabric thickness, however, SEM images show better penetration of the silicone into the yarns at a higher add-on (Figure 1).

**Table 1.** Details of mass per unit area and silicone add-on ( $W_C - W_{UC}$ ) of un-sized and plasma-treated basalt fabrics coated with different silicone content (CR (%)).

Sample	$W_{UC}$ ( $\text{g}/\text{m}^2$ )	$W_C$ ( $\text{g}/\text{m}^2$ )	$W_C - W_{UC}$ ( $\text{g}/\text{m}^2$ )	CR (%)	Thickness mm ( $\pm$ std)	
Un-sized	Basalt 1	203	203	0	–	
	Basalt 2	192	400	208	108	
	Basalt 3	203	522	319	157	
	Basalt 4	206	563	357	173	0.5 (0.1)
	Basalt 5	207	745	538	261	0.6 (0.1)
Plasma-treated	Basalt 6	203	575	372	183	0.6 (0.05)
	Basalt 7	207	591	384	186	–
	Basalt 8	201	637	436	217	–
	Basalt 9	198	705	507	256	0.6 (0.06)
	Basalt 10	201	783	582	289	–
	Basalt 11	203	203	0	0	–

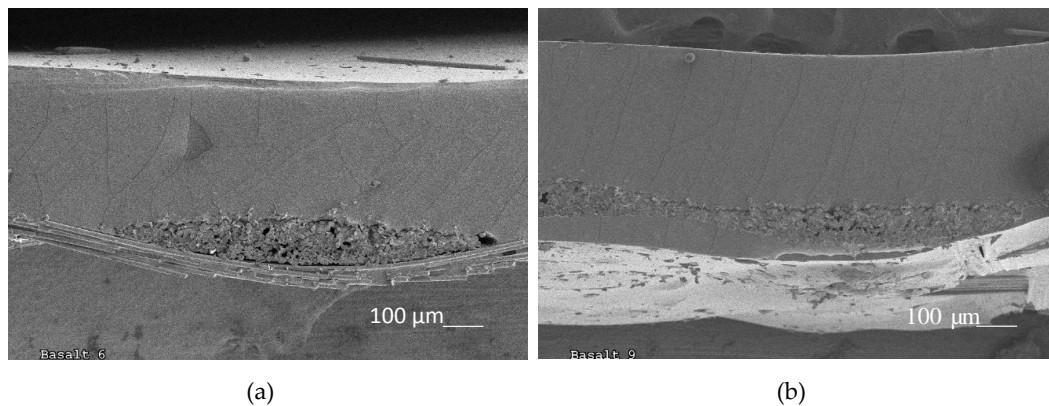


**Figure 1.** Scanning electron microscopy (SEM) images of (a) Basalt 6 and (b) Basalt 9 sections showing greater penetration of the silicone into the fabric at a higher add-on.

Heat transfer results for the un-sized fabrics coated with silicone are shown in Table 2. Un-sized fabric with no silicone-elastomer (Basalt 1,  $t_{24} = 8.4 < 11$  s and  $t_{24} - t_{12} = 3.2 < 4$  s) does not satisfy the standard requirements for fire-fighting protective apparel, though  $T_F$  is less than 70%. After coating, regardless of the silicone add-on ( $W_c - W_{uc}$ ), an improvement in thermal resistance ( $t_{24} > 11$  s and  $T_F \leq 70\%$ ) is observed. However, only Basalt 4 (CR of 173%) and Basalt 5 (CR of 261%) fabrics met the minimum requirements for heat transfer of protective apparel. As expected, increasing the silicone add-on increased  $t_{24} - t_{12}$  and decreased  $T_F$  as heat transfer through the fabric became more difficult. Increasing the silicone add-on showed improvement in the thermal resistance ( $1/Q_C$ ).

**Table 2.** Heat transfer parameters of un-sized basalt fabrics coated with different silicone content (CR (%)).

Sample	CR (%)	$t_{12}$ (s)	$t_{24}$ (s)	$t_{24} - t_{12}$ (s)	$T_F$ (%)	$Q_C$ (KW/m <sup>2</sup> )
Basalt 1	0	5.2	8.4	3.2	51.8	20.7
Basalt 2	108	16.7	20.2	3.5	47	18.9
Basalt 3	157	17.8	21.7	3.9	42	17.0
Basalt 4	173	15.5	19.6	4.1	40	16.2
Basalt 5	261	17.8	22.6	4.8	35	13.8

The results of the heat transfer assessments for the plasma-treated fabrics coated with silicone are shown in Table 3. The samples have been coated with silicone with a CR% ranging from 183% to 289%. Our observations showed that coating silicone on un-sized fabric at a higher add-on and even thickness was not easy to achieve as the silicone did not easily spread on the surface of the fabric. After plasma-treatment, coating onto the fabric was easier and a uniform surface on both sides of the fabric with a higher add-on, up to 289%, was achieved (Table 3, Basalt 10). As shown in Table 3, after plasma-treatment, the increasing silicone add-on led to an improvement in heat transfer resistance. All of the coated, plasma-treated samples met the minimum requirements for heat transfer of protective apparel [29].

As shown in Table 3,  $T_F$  reduced to 35% at a CR of 183% (Basalt 6). However, a CR of 261% was required to achieve the same  $T_F$  on the un-sized fabrics without pre-plasma treatment (Basalt 5, Tables 1–3). Basalt 6 (plasma-/silicone-coated fabric) required a lower add-on of silicone to achieve similar heat transfer velocity and heat transfer performance compared to Basalt 5 (un-sized/silicone-coated fabric). Comparing Basalt 5 and Basalt 9 with relatively similar silicone content (CR), confirmed that plasma treatment prior to silicone coating improved the heat transfer resistance of the fabric. While un-sized fabric, Basalt 5 with 261% silicone content, showed a  $T_F$  of

35% and  $Q_C$  of 13.8 kW/m<sup>2</sup>, similar silicone content (Basalt 9, CR = 256%) after plasma treatment significantly reduced the  $T_F$  to 24% and  $Q_C$  to 9.6 kW/m<sup>2</sup>. The results suggest a possible synergistic effect between the plasma treatment and silicone coating, confirming that plasma treatment reduced the amount of silicone required, yet improved the heat transfer resistance of the fabric. The lower silicone content will reduce the weight of the coated fabric and improve the performance of protective clothing. Otherwise, without plasma treatment multilayer fabrics or more silicone will be required.

**Table 3.** Heat transfer parameters of plasma-treated basalt fabrics coated with different silicone contents (CR (%)).

Sample	CR (%)	$t_{12}$ (s)	$t_{24}$ (s)	$t_{24}-t_{12}$ (s)	$T_F$ %	$Q_C$ (kW/m <sup>2</sup> )
Basalt 6	183	17.7	22.4	4.7	35	14.1
Basalt 7	186	17.7	23.1	5.4	31	12.3
Basalt 8	217	17.5	23.1	5.6	30	11.8
Basalt 9	256	17.4	24.3	6.9	24	9.6
Basalt 10	289	17.7	26.6	8.9	19	7.4

### 3.2. Surface Morphology and Cross-Section Analysis

The SEM images of un-sized (Basalt 1) and plasma-treated (Basalt 11) single fibres that were pulled from the fabrics are shown in Figure 2a,b. The images clearly showed that the fibre surface morphology changed following the plasma treatment. While the un-sized sample showed a smooth and even surface, the plasma-treated sample showed some protrusions and grooves on the surface of the fibres as results of plasma etching. After plasma treatment, the surface roughness increased, which increased the surface area of the fibre. These results are consistent with the morphology of plasma-treated polypropylene fibre, as reported by Yaman et al. [30].

A three-dimensional SPM surface morphology of basalt and plasma-treated fibres shows further microscopic changes on the fibre surface, as shown in Figure 3a,b. The surface morphology of the un-sized fibre is relatively flat, clean, and smooth, which is consistent with the SEM images Figure 2a and the nature of the basalt fibre. An increase in roughness of the plasma-treated fibre can be seen in Figure 3, relative to the un-sized fibre. The surface roughness of the un-sized fibre varied between 5.43 to 10.1 nm (with an average of 5.62 nm and a root mean square of 6.25 nm), whereas that of the plasma-treated fibre varied between 15.9 and 25.9 nm (with an average of 22.3 nm and a root mean square of 28.6 nm). Consistent with the SEM images, an increase in surface area and interlocking between the fibre/silicone-elastomer interfaces could be expected after plasma treatment [31].

The SEM images of single fibres pulled out from un-sized basalt fabrics coated with silicone (Basalt 4,5) and pre-treated samples with plasma then coated with silicone (Basalt 6,9) are shown in Figure 2c,e and Figure 2d,f, respectively. The cross-section images of the corresponding samples are also shown in Figure 4. These images suggested that the silicone polymer is more evenly spread (especially between fibres) on the fabrics that were pre-treated with plasma before polymer treatment, compared to fabrics with no plasma treatments.

The plasma-treated samples also showed more silicone coverage over and between the fibre surfaces compared to un-sized samples. The rougher surface produced on the surface of the plasma-treated fibres, as evidence by Figures 2b and 3b, may help to anchor the polymer onto and between the fibre surfaces and increase the amount of silicone coated on the fibre surface. This has been further supported by the higher value calculated for CR (%) on the plasma-treated samples compared to un-sized fabric (Table 1) coated with the same blade height. The penetration of silicone into the voids may be the reason for the improvement in heat transfer resistance of the plasma-treated basalt fabrics compared to the un-sized fabrics (Tables 2 and 3).

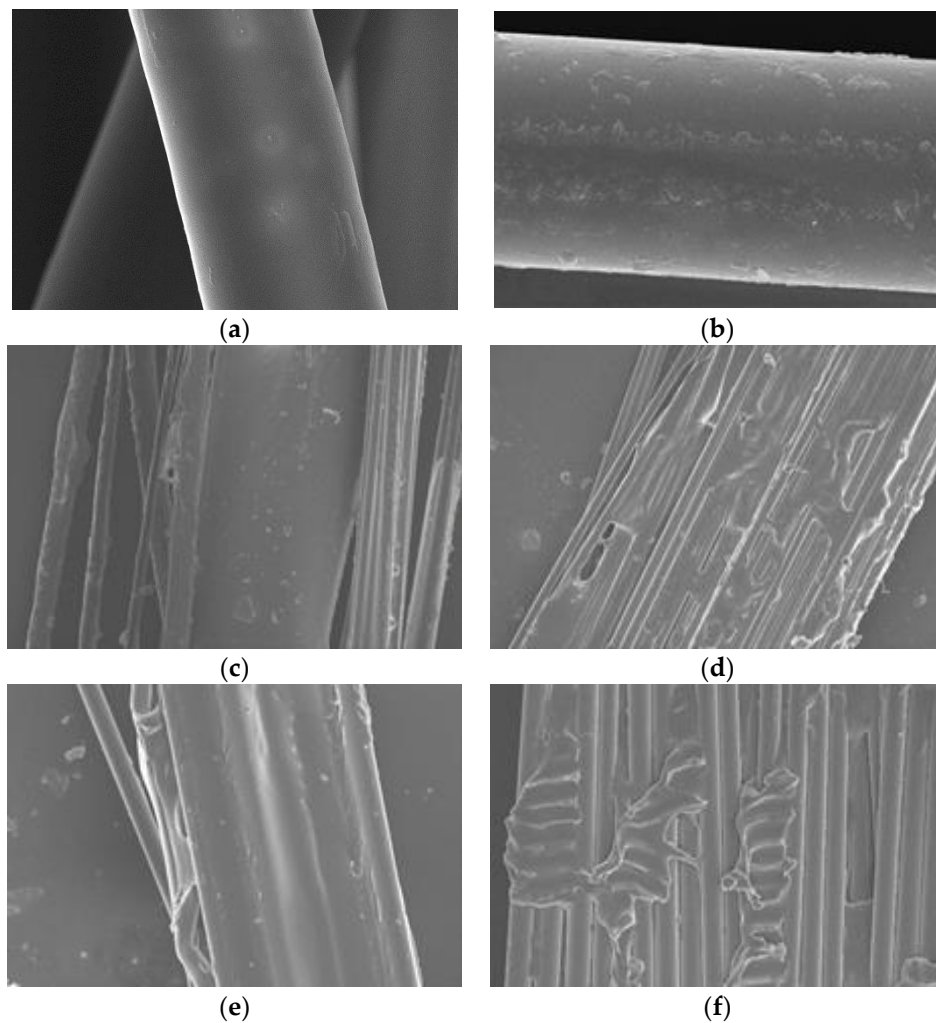


**Figure 2.** SEM images of basalt fibres: (a) un-sized (Basalt 1), and (b) plasma-treated (Basalt 11); (c) un-sized/silicone-coated CR 173% (Basalt 4); (d) plasma-treated/silicone-treated CR 183% (Basalt 6); (e) un-sized/silicone-coated CR 261% (Basalt 5); (f) plasma-treated/silicone-coated CR 256% (Basalt 9).

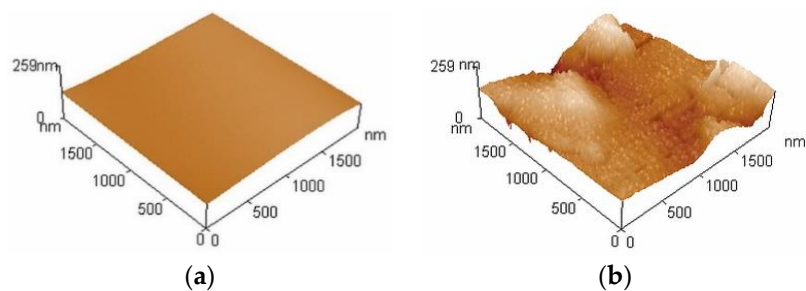


**Figure 3.** Scanning probe microscopy (SPM) analysis of basalt fibres: (a) un-sized fibre (Basalt 1), and (b) plasma-treated fibre (Basalt 11).

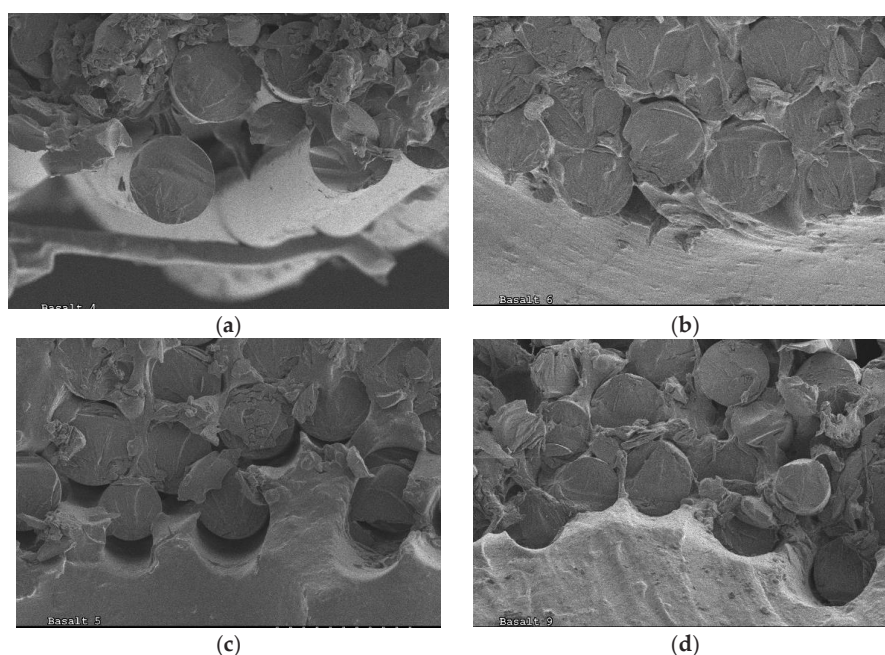


**Figure 4.** Cross-sectional images of basalt fibres: (a) un-sized/silicone-coated CR 173% (Basalt 4); (b) plasma-treated/silicone-treated CR 183% (Basalt 6); (c) un-sized/silicone-coated CR 261% (Basalt 5); (d) plasma-treated/silicone-coated CR 256% (Basalt 9).

### 3.3. XPS Analysis

The relative atomic concentrations of carbon, nitrogen, oxygen, and silicon in the surface of un-sized and plasma-treated basalt fabrics are shown in Table 4. In order to further characterise the changes in surface chemistry resulting from plasma treatment, different components were fitted to the high-resolution C 1s region spectra, as shown in Figure 5 and Table 4.

**Table 4.** Atomic concentration (%) of the elemental surface composition and relative atomic concentration of carbon for basalt fabrics treated with plasma.

Fabric Sample	Elements				Carbon Compositions (C 1s %)		
	C 1s 284.80 eV	N 1s 399.37 eV	O 1s 532.11 eV	Si 2p 102.13 eV	C1 (C–C, C–Hx) 284.13 eV	C2 (C–O, C–O–C) 285.68 eV	C3 (O–C–O, N–C=O) 287.12 eV
Un-sized (Basalt 1)	68.87	0.66	25.02	4.79	58.2	38.3	3.5
Plasma-treated (Basalt 11)	33.27	0.6	47.04	14	41.3	44.4	14.3

Plasma-treated fabric showed a significant decrease in the carbon content to half of the original carbon concentration. A significant increase in the oxygen concentration (almost twice as high) was found for the plasma-treated fabric compared with the un-sized fabric. While the nitrogen atomic concentration remained unchanged after plasma treatment, the Si 2p content was enhanced almost three times.

The C 1s high-resolution spectra is showed in Figure 4. Three components were fitted to the original curve. According to the binding energy, the peak at about 284.13 eV is typical of carbon without oxygen bonds and is only bound to carbon and hydrogen C1 (C–C, C–Hx). The peak at higher bonding energy (285.68 eV) is typical of carbon single bond to oxygen and or nitrogen C2 (C–O, C–O–C), and the peak near 287.12 eV corresponds to carbon with two oxygen and/or nitrogen bonds C3 (O–C–O, N–C=O) [32].

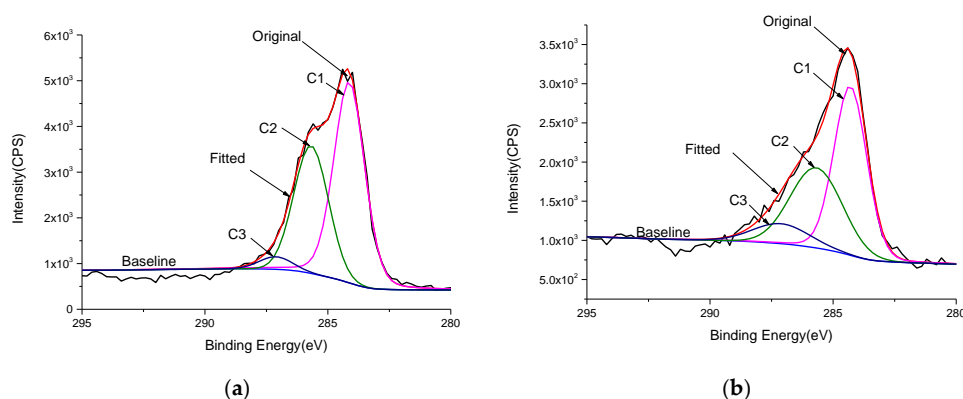


**Figure 5.** High-resolution XPS C 1s spectra: (a) un-sized basalt fabric (Basalt 1), and (b) plasma-treated basalt fabric (Basalt 11).

After plasma treatment, a reduction in the content of non-polar groups of C–C and an increase in the content of polar groups of carbon/oxygen (C–O and C=O) was observed. Carbon bound to two oxygen (C3) increased almost three times as much after plasma treatment. Considering the preparation conditions and elemental components of basalt fibre, the changes in the content of the polar groups is consistent with the plasma treatment using oxygen gas, oxidizing the residual hydrocarbon on the basalt fibre surface. Consistent with the increased polarity of the surface observed in the XPS results, an increase in bonding between fibres and silicone could be expected after plasma treatment, as suggested by the SEM cross-section images.

#### 3.4. Water Absorption Assessments

Water contact angle and absorption time of un-sized (Basalt 1) and plasma-treated fabrics (Basalt 11) are shown in Table 5. The Work of adhesion calculated from the contact angle data has also been used to estimate the surface energy of the fibres. The un-sized basalt fabric showed a hydrophobic nature, consistent with the presence of a hydrocarbon layer on the surface. After the plasma treatment, the contact angle reduced from 109° to 47° and the fabric became hydrophilic, with an absorption time of 1.6 sec compared to 39 s for the un-sized fabric. As expected, after plasma treatment the work of adhesion increased (almost 2.5 times as much).

**Table 5.** Results of wettability assessments of un-sized and plasma-treated basalt fabric.

Sample	Contact Angle (° ± std <sup>a</sup> )	Absorption Time (sec ± std <sup>a</sup> )	Work of Adhesion (mJ/m <sup>-2</sup> )	The Image of the Contact Angle
Un-sized (Basalt 1)	109 (±5)	39 (±9)	49.03	
Plasma-treated (Basalt 11)	47 (±3)	1.6 (±0.3)	122.37	

<sup>a</sup> standard deviation of three measurements.

Wettability is a necessary condition for resin bonding [33], therefore, the higher surface energy of plasma-treated basalt fabric compared to un-sized fabric may explain the higher silicone content of plasma-treated fabrics compared to un-sized fabrics (Table 1). The results are in agreement with a previous study where basalt/epoxy woven composites were treated with oxygen plasma [19]. The higher wettability of the plasma-treated basalt fibre can be attributed to the oxidation of the treated surface and the greater roughness and surface area resulting from etching by the plasma treatment. All these effects may result in increasing the work of adhesion and the spreading of the silicone into the yarns.

#### 4. Conclusions

The effect of plasma treatment prior to silicone coating and its effect on the adsorption of silicone onto basalt fabric were investigated using different analytical techniques. SEM and SPM observations confirmed that surface roughness and surface area after plasma treatment both increased. XPS analysis showed the presence of a hydrocarbon layer on the un-sized fibre, and that plasma treatment considerably oxidized this hydrocarbon on the basalt fibre surface, which was in agreement with a lower water contact angle and shorter water absorption times of plasma-treated basalt fabrics. Silicone coating after plasma pre-treatment showed a more uniform spread of silicone on the surface and a higher add-on of silicone-elastomer between fibres compared to samples without plasma treatment.

Different add-ons of silicone-elastomer were applied on the un-sized and plasma-treated basalt fabrics. In general, a higher percentage of silicone reduced the rate of thermal transfer from a radiant heat source. The etching and roughening of the surface by plasma treatment of the basalt fibres improved the evenness of the silicone coating and reduced the add-on of silicone required to satisfy the standard requirement of heat transfer through protective clothing.

**Author Contributions:** Data Curation, Y.S.; Investigation, M.Z. and Z.Z.; Methodology, M.Z., R.D., and M.N.; Supervision, M.N.; Validation, M.Z., R.D., and M.N.; Writing—Original Draft Preparation, M.Z.; Writing—Review and Editing, R.D., X.W. and M.N.

**Funding:** This research was funded by the Tianjin Research Program of Application, Foundation, and Advanced Technology [13JCYBJC16800]; the China National Funds for Distinguished Young Scientists [51303131], and the China National Funds for Distinguished Young Scientists [61307094].

**Acknowledgments:** The China Scholarship Council (CSC) is gratefully acknowledged. Deakin University is acknowledged for visiting support provided for the first author of this paper.

**Conflicts of Interest:** The authors declare no conflict of interest. The funders had no role in the design of the study; in the collection, analyses, or interpretation of data; in the writing of the manuscript, and in the decision to publish the result.

#### References

1. Carmisciano, S.; De Rosa, I.M.; Sarasini, F.; Tamburrano, A.; Valente, M. Basalt woven fiber reinforced vinylester composites: Flexural and electrical properties. *Mater. Des.* **2011**, *32*, 337–342. [[CrossRef](#)]
2. Bhat, T.; Chevali, V.; Liu, X.; Feih, S.; Mouritz, A.P. Fire structural resistance of basalt fibre composite. *Compos. Part A Appl. Sci. Manuf.* **2015**, *71*, 107–115. [[CrossRef](#)]
3. Fiore, V.; Scalici, T.; Di Bella, G.; Valenza, A. A review on basalt fibre and its composites. *Compos. Part B Eng.* **2015**, *74*, 74–94. [[CrossRef](#)]
4. Wu, Z.; Wang, X.; Wu, G. Advancement of basalt fiber composites towards infrastructural applications. In Proceedings of the International Symposium on Innovation & Sustainability of Structures, Xiamen, China, October 28–30 2011.
5. Lopresto, V.; Leone, C.; De Iorio, I. Mechanical characterisation of basalt fibre reinforced plastic. *Compos. Part B Eng.* **2011**, *42*, 717–723. [[CrossRef](#)]
6. Meng, Q.; Hao, H.; Chen, W. Experimental and numerical study of basalt fibre cloth strengthened structural insulated panel under windborne debris impact. *J. Reinf. Plast. Compos.* **2016**, *35*, 1302–1317. [[CrossRef](#)]
7. Cai, J.; Pan, J.; Zhou, X. Flexural behavior of basalt FRP reinforced ECC and concrete beams. *Constr. Build. Mater.* **2017**, *142*, 423–430. [[CrossRef](#)]
8. Katkhuda, H.; Shatarat, N. Improving the mechanical properties of recycled concrete aggregate using chopped basalt fibers and acid treatment. *Constr. Build. Mater.* **2017**, *140*, 328–335. [[CrossRef](#)]
9. Tkachev, S.V.; Kraevskii, S.V.; Kornilov, D.Y.; Voronov, V.A.; Gubin, S.P. Graphene oxide on the surface of basalt fiber. *Inorg. Mater.* **2016**, *52*, 1254–1258. [[CrossRef](#)]
10. Shishevan, F.A.; Akbulut, H.; Mohtadi-Bonab, M.A. Low velocity impact behavior of basalt fiber-reinforced polymer composites. *J. Mater. Eng. Perform.* **2017**, *26*, 2890–2900. [[CrossRef](#)]
11. Medvedyev, O.; Tsybulya, Y. Basalt use in hot gas filtration. *Filtr. Sep.* **2005**, *42*, 34–37. [[CrossRef](#)]
12. Pang, Y.; Zhong, Z.L.; Liu, H.W.; Rao, L.K. Research on fire-resistant fabric properties of basalt fiber. *Appl. Mech. Mater.* **2012**, *217*, 1151–1154. [[CrossRef](#)]

13. Li, C.; Gao, D.; Wang, Y.; Tang, J. Effect of high temperature on the bond performance between basalt fibre reinforced polymer (BFRP) bars and concrete. *Constr. Build. Mater.* **2017**, *141*, 44–51. [[CrossRef](#)]
14. Lu, Z.; Xian, G.; Li, H. Effects of elevated temperatures on the mechanical properties of basalt fibers and BFRP plates. *Constr. Build. Mater.* **2016**, *127*, 1029–1036. [[CrossRef](#)]
15. Manikandan, V.; Jappes, J.W.; Kumar, S.S.; Amuthakkannan, P. Investigation of the effect of surface modifications on the mechanical properties of basalt fibre reinforced polymer composites. *Compos. Part B Eng.* **2012**, *43*, 812–818. [[CrossRef](#)]
16. Zille, A.; Oliveira, F.R.; Souto, A.P. Souto Plasma treatment in textile industry. *Plasma Process. Polym.* **2015**, *12*, 98–131. [[CrossRef](#)]
17. Najar, S.S.; Wang, X.; Naebe, M. The effect of plasma treatment and tightness factor on the low-stress mechanical properties of single jersey knitted wool fabrics. *Text. Res. J.* **2016**, *88*, 499–509. [[CrossRef](#)]
18. Kurniawan, D.; Kim, B.S.; Lee, H.Y.; Lim, J.Y. Atmospheric pressure glow discharge plasma polymerization for surface treatment on sized basalt fiber/polylactic acid composites. *Compos. Part B Eng.* **2012**, *43*, 1010–1014. [[CrossRef](#)]
19. Kim, K.Y.R.; Park, S.J. Plasma treatment and its effects on the tribological behaviour of basalt/epoxy woven composites in a marine environment. *Polym. Polym. Compos.* **2011**, *19*, 29–34.
20. Antonova, M.V.; Krasina, I.V.; Ilyushina, S.V.; Mingaliev, R.R.; Parsanov, A.S. Modification of basalt fibers by low-temperature plasma. *J. Phys. Conf. Ser.* **2018**, *1058*, 012003. [[CrossRef](#)]
21. Kim, M.T.; Kim, M.H.; Rhee, K.Y.; Park, S.J. Study on an oxygen plasma treatment of a basalt fiber and its effect on the interlaminar fracture property of basalt/epoxy woven composites. *Compos. Part B Eng.* **2011**, *42*, 499–504. [[CrossRef](#)]
22. Hrynyk, R.; Frydrych, I.; Irzmańska, E.; Stefko, A. Thermal properties of aluminized and non-aluminized basalt fabrics. *Text. Res. J.* **2012**, *83*, 1860–1872. [[CrossRef](#)]
23. Hrynyk, R.; Frydrych, I. Study on textile assemblies with aluminized basalt fabrics destined for protective gloves. *Int. J. Cloth. Sci. Technol.* **2015**, *27*, 705–719. [[CrossRef](#)]
24. *ISO 15384-2003 Protective Clothing for Firefighters-Laboratory Test Methods and Performance Requirements for Wildland Firefighting Clothing*; ISO: Geneva, Switzerland, 2003.
25. *ISO 11613-2017 Protective Clothing for Firefighter's Who are Engaged in Support Activities Associated with Structural Fire Fighting-Laboratory Test Methods and Performance*; ISO: Geneva, Switzerland, 2017.
26. *MS ISO 15538-2005 Protective Clothing for Firefighters-Laboratory Test Methods and Performance Requirements for Protective Clothing with a Reflective Outer Surface*; ISO: Geneva, Switzerland, 2005.
27. *EN ISO 6942-2002 Protective Clothing —Protection against Heat and Fire—Method of Test: Evaluation of Materials and Material Assemblies when Exposed to A Source of Radiant Heat*; ISO: Geneva, Switzerland, 2002.
28. Naebe, M.; Cookson, P.G.; Denning, R.; Wang, X. Use of low-level plasma for enhancing the shrink resistance of wool fabric treated with a silicone polymer. *J. Text. Inst.* **2011**, *102*, 948–956. [[CrossRef](#)]
29. Naebe, M.; Cookson, P.G.; Rippon, J.; Brady, R.P.; Wang, X.; Brack, N.; van Riessen, G. Effects of plasma treatment of wool on the uptake of sulfonated dyes with different hydrophobic properties. *Text. Res. J.* **2009**, *80*, 312–324. [[CrossRef](#)]
30. Yaman, N.; Özdoğan, E.; Seventekin, N.; Ayhan, H. Plasma treatment of polypropylene fabric for improved dyeability with soluble textile dyestuff. *Appl. Surf. Sci.* **2009**, *255*, 6764–6770. [[CrossRef](#)]
31. Naebe, M.; Denning, R.; Huson, M.; Cookson, P.G.; Wang, X. Ageing effect of plasma-treated wool. *J. Text. Inst.* **2011**, *102*, 1086–1093. [[CrossRef](#)]
32. Naebe, M.; Li, Q.; Onur, A.; Denning, R. Investigation of chitosan adsorption onto cotton fabric with atmospheric helium/oxygen plasma pre-treatment. *Cellulose* **2016**, *23*, 2129–2142. [[CrossRef](#)]
33. Salapare, H.S.; Darmanin, T.; Guittard, F. Reactive-ion etching of nylon fabric meshes using oxygen plasma for creating surface nanostructures. *Appl. Surf. Sci.* **2015**, *356*, 408–415. [[CrossRef](#)]

